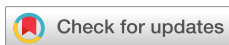


RESEARCH ARTICLE | DECEMBER 27 2023

## Metallic hydrogen: Study of metastability

W. C. Ferreira  ; M. Møller  ; K. Linsuain; J. Song  ; A. Salamat  ; R. Dias  ; I. F. Silvera 



APL Mater. 11, 121116 (2023)

<https://doi.org/10.1063/5.0178261>

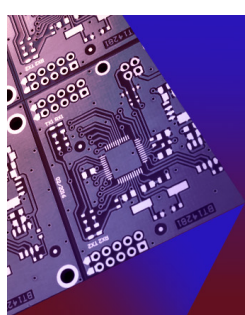


View  
Online



Export  
Citation

CrossMark



**APL Electronic Devices**

**CALL FOR APPLICANTS**

**Seeking Editor-in-Chief**

 **AIP  
Publishing**

# Metallic hydrogen: Study of metastability

Cite as: APL Mater. 11, 121116 (2023); doi: 10.1063/5.0178261

Submitted: 26 September 2023 • Accepted: 14 November 2023 •

Published Online: 27 December 2023



View Online



Export Citation



CrossMark

W. C. Ferreira,<sup>1</sup>  M. Møller,<sup>1</sup>  K. Linsuain,<sup>1</sup> J. Song,<sup>1,a)</sup>  A. Salamat,<sup>2</sup>  R. Dias,<sup>3</sup>  and I. F. Silvera<sup>1,b)</sup> 

## AFFILIATIONS

<sup>1</sup> Lyman Laboratory of Physics, Harvard University, Cambridge, Massachusetts, USA

<sup>2</sup> Department of Physics and Astronomy, University of Las Vegas, Las Vegas, Nevada, USA

<sup>3</sup> Department of Physics and Astronomy, University of Rochester, Rochester, New York, USA

<sup>a)</sup>**Current address:** Institute of Physics, Chinese Academy of Sciences, Beijing 100190, China.

<sup>b)</sup>**Author to whom correspondence should be addressed:** [silvera@physics.harvard.edu](mailto:silvera@physics.harvard.edu)

## ABSTRACT

Metallic hydrogen (MH) has been predicted to be metastable, a high temperature superconductor, and a powerful rocket propellant. If true, MH could have an enormous impact on society. We have produced MH in a diamond anvil cell and studied its metastability. At a temperature of 5 K, the load on the metallic hydrogen was stepwise reduced until the pressure was essentially zero. While turning the load or pressure down, the sample evidently transformed to the molecular phase and escaped; the hole in the gasket containing the MH closed. We were unable to determine this value of the metastability pressure. Metallic hydrogen was not observed to be metastable at zero pressure, with no uncertainty.

© 2023 Author(s). All article content, except where otherwise noted, is licensed under a Creative Commons Attribution (CC BY) license (<http://creativecommons.org/licenses/by/4.0/>). <https://doi.org/10.1063/5.0178261>

## I. INTRODUCTION

### A. Metastability

In this paper, we study metallic hydrogen (MH) at high pressures and low temperatures in a diamond anvil cell (DAC). After producing MH in the laboratory, we studied the possibility that it is metastable, or answer the question “Will MH remain metallic when the ultra-high pressure needed to produce it is lifted, or will it convert back to molecular hydrogen?”.

If MH exists under ambient conditions and is superconducting, it would be revolutionary, with applications having a large impact on society.<sup>1</sup> Metastability of MH was first proposed over 50 years ago by Brovman *et al.*<sup>2</sup> They carried out a detailed calculation of the energy and equation of state, including possible structures, using perturbation theory in the low temperature limit. They found that the ground state could be a liquid, or an array of protonic filaments (one dimensional chains), yet a stable metal at low pressures. They considered the effect of zero-point motion (ZPM) and realized that metallic deuterium with a much smaller ZPM had distinct advantages for metastability, compared to hydrogen. They also considered that a short lifetime of the metastable phase might limit its usefulness. If the ground state was a liquid, it would have fundamental implications: liquid MH might have novel quantum states, with both superfluidity and superconductivity.<sup>3</sup>

A recent discussion of the metastability of hydrogen, with an extensive list of references, is provided by Tenney *et al.*<sup>4</sup> They carried

out a first-principles analysis of this problem using density functional theory. There are two considerations for metastability: One must first find the metastability pressure  $P_m$  in the low temperature limit. If the sample is metastable at ambient pressure, then the temperature should be increased until thermal dynamics causes a transition to molecular hydrogen at the temperature  $T_m$ . For example, diamond is a metastable phase of carbon.  $P_m$  is zero atm.; however, if heated to a temperature  $T_m \approx 1400$  K, diamond will convert to the low energy phase, i.e., graphite. Tenney *et al.* found  $P_m \approx 200$  GPa for MH. Burmistrov and Dubovskii<sup>5</sup> predicted stability down to 10–20 GPa, while Ackland<sup>6</sup> found MH to be unstable at 0 atm. Clearly, it is important to experimentally determine  $P_m$  and  $T_m$  for hydrogen. In the present experiment, we considered  $T \approx 5$  K to be in the low temperature limit.

To observe metastability, our plan was to load hydrogen in a DAC, make MH, and confirm this by measuring reflectance at low temperatures. Then, at a sample temperature of 5 K, we would slowly release the load while visually observing the sample. If it remained in the gasket hole at effectively zero pressure, then it is metastable; if it disappeared, it is not.

### B. Metallic hydrogen

There are two thermodynamic pathways for making metallic hydrogen, with different end points. Pathway I is a low-temperature very high-pressure pathway, and pathway II is a high-temperature

pathway at intermediate pressures (see the phase diagram in the supplementary material) (Fig. S1 from Ref. 7). Pathway II includes a first-order phase transition to liquid atomic metallic hydrogen. The phase line for the latter was observed by Zaghou *et al.*<sup>8</sup> at pressures of order 100–200 GPa and temperatures of 1000–2000 K. Pathway II is not of relevance for this paper as the high temperature phase has only been created by pulsed techniques and is very short-lived.

Pathway I is the focus of this paper. In 1935, Wigner and Huntington<sup>9</sup> predicted that at a sufficiently high density or pressure, solid molecular hydrogen would transition to atomic metallic hydrogen by molecular dissociation. This insulator to metal transition was first observed in the laboratory by Dias and Silvera<sup>10</sup> at a pressure reported as  $495 \pm 13$  GPa at temperatures of  $\sim 5$  K and 83 K. They increased the pressure in steps, while observing the sample to transition from transparent to an opaque black molecular phase and, finally, to shiny MH, surrounded by the less reflective rhenium (Re) gasket, as shown in Fig. S2 for visible wavelengths. The reflectance was measured as a function of wavelength and fit to a Drude free-electron model of a metal that yields the plasma frequency or the electron density. It was found to be a metal with one electron per proton or atomic metallic hydrogen.

This first observation of the Wigner–Huntington transition to atomic MH was met with comments and objections but all could be answered.<sup>11</sup> Significant comments were that the experiment on MH should be repeated and that the Drude model should be fit for more than two wavelengths. Here, we set out to respond in two ways: measure the reflectance of MH (the subject of this paper) and measure the electrical conductivity of MH. The reflectance was measured at Harvard, and the conductivity was measured at the University of Rochester.<sup>12</sup> In the latter, the transition pressure was measured to be 470–480 GPa, using the shift of the Raman active phonon in the diamond, currently the best method of determining ultra-high pressures in DACs. This agrees with the pressure determined by Dias and Silvera. In the present paper, we measured the reflectance at five wavelengths in the visible/infrared, confirming the metallic behavior of hydrogen. We have had a few other observations in which MH was produced. For technical reasons, nothing new was measured, so the resulting repeated observations of MH were not published, except to show photos of the MH phase.<sup>13</sup> Producing MH requires enormous pressures, challenging the structural integrity of the diamonds. In one of those productions of MH, the diamonds failed before new measurements could be completed; in the other, internal damage in one of the diamonds prevented measurement of the pressure. It turns out that strong laser beam intensity, used for Raman scattering studies, can damage the diamond, leading to failure, and should be limited (see ahead).

## II. EXPERIMENTAL METHODS

### A. Pressure determination

A crucial point is the determination of the pressure. At very high pressures of concern (up to  $\sim 500$  GPa), pressure is determined by measuring the calibrated shift<sup>14</sup> of the Raman active diamond phonons in the stressed part of the diamond (the culet region), while at intermediate pressures, the calibrated shift of the infrared active vibron is used. Unfortunately, the Raman pressure determination can lead to failure of the diamonds. In 1998, Narayana

*et al.*<sup>15</sup> studied hydrogen to 342 GPa using Raman scattering of the hydrogen vibron to determine the pressure. Fifteen sets of diamonds were broken in total, every time the stressed diamonds were illuminated with laser light used for Raman scattering (Ruoff, Pvt. Comm. to Silvera). We have our own experience in measuring the Raman shift of the diamond; in this case, we found that the higher the pressure, the lower the laser power at which the diamonds fail, as shown in Fig. S3. Thus, at a pressure of  $\sim 500$  GPa,  $\sim 1$  mW of laser power is sufficient to cause damage to the diamond. We have found that such diamond failure also depends on how long the diamond has been under stress. In the first experiment on making MH,<sup>10</sup> the metallization pressure ( $\sim 500$  GPa) was successfully measured with  $\sim 20$  mW of laser power, whereas some months later, an attempt to measure the pressure with 0.5 mW led to catastrophic failure of the diamonds. Evidently, the defect density (vacancies, etc.) develop in the stressed region and the light interacts with the defects.

For this study, if the diamonds fail, the experiment would be terminated; then, the possible metastability of MH would not be observable even though the sample was shown to be metallic. Thus, we decided to preclude a Raman measurement of the stressed part of the diamond to determine the pressure and use another technique. With our DACs,<sup>16</sup> we can continuously raise the pressure by turning a drive screw to increase the load on the gasket and sample. Our DACs are also provisioned with calibrated strain gauges that indicate the load or force. We have found in many previous runs that the measured pressure of the sample is proportional to the rotation of the drive screw or the load; that is, there is a linear relationship between the load (or the rotation of the screw) and the pressure. Our DAC, which we have used many times before, obeys this linear relationship. In Fig. S4, we show a plot of the pressure measured using the calibrated shift of the IR active vibron vs load, or turns of the screw to increase the load. The calibration, discussed in the supplementary material of Ref. 1, is  $P = [4701.21 - (\omega \text{ cm}^{-1})]/[1.92389]$  GPa, where  $\omega$  is the peak of the IR vibron, and we extrapolate this to higher pressure, counting the number of turns of the drive screw (Fig. S4). For all of our measurements and photos of the sample, we indicate the number of turns of the drive screw in eighths of a turn, from which the pressure is determined; we also record the load from the strain gauge. Using this extrapolation, we find the pressure of metallization in this experiment to be between 477 and 492 GPa, in agreement with the observation of Dias and Silvera. When the load is lowered (turning the screw back), the pressure is reduced. The uncertainty of about 15 GPa has several sources, including the extrapolation of the IR vibron data, the fitting of the diamond Raman phonon shift data<sup>14</sup> estimated to have a few percent uncertainty, and the sampling intervals chosen for increases in the load. We note that in reducing the load, the linear fit of Fig. S4 is not applicable and will be discussed ahead.

### B. Diamonds and loading

We cryogenically loaded 0.9999 pure hydrogen in a DAC. The diamonds were conic type II as, with  $30 \mu\text{m}$  culet flats and a  $9^\circ$  bevel with a diameter of  $300 \mu\text{m}$ . As mentioned above, some of our results are from visual observation of the sample. We used two microscopes in this study. The Leitz microscope was used for the preparation

of DACs at room temperature, with a magnification of a few hundred. For viewing the sample in the cryostat (which has 3  $\text{CaF}_2$  windows intervening), we used a Wild macroscope, with a high quality long-working distance objective (120 mm) with a magnification of 30 to 40.

The pre-indented gasket was made of rhenium, with a  $19 \mu\text{m}$  diameter sample hole and a thickness of  $10 \mu\text{m}$  under the culet. The gasket was gold coated before indenting to minimize stress induced damage to the diamonds when pre-indenting. The hole was made by electric discharge machining (EDM); this leaves a ring of black slag (melted and redeposited metal) around the edge of the hole [see Fig. 1(a)]. Our usual procedure is to use high-power ultrasonics on the gasket submerged in water mixed with micron-sized alumina particles; this removes the gold but not the slag. The slag is then knocked off using a sharpened toothpick, viewing through the macroscope. The diamonds and gasket are then coated with a 50 nm layer of alumina using atomic layer deposition. This protects the diamonds from hydrogen diffusion and embrittlement, while the Re gasket is protected from interacting with hydrogen to form rhenium hydride.

This last step to remove the slag was inadvertently skipped and only noticed after the DAC was cooled to liquid helium temperatures. Due to the limited supply of liquid helium (at that time), we decided to proceed with loading of hydrogen. We do cryogenic loading by filling a sealed mini-chamber enclosing the diamonds and gasket with liquid hydrogen. During loading, some of the slag was crushed between the two diamonds. The slag spread out over the rhenium, leaving a possibly rough surface. During loading, the slag on the surface could cause leakage of the hydrogen until fully flattened until the sample was sealed in the gasket hole. When this occurred, the hole diameter was about  $10.8 \mu\text{m}$  rather than closer to the initial diameter of  $19 \mu\text{m}$ , resulting in a smaller than desired initial sample diameter. The black slag smeared out on the Re but did not enter the hole or the hydrogen. When the sample was viewed through a microscope, one observed a transparent sample

surrounded by the black slag rather than surrounded by the reflective rhenium [see Fig. 1(b)]. We carefully tracked the sample dimensions with increasing pressure. The sample shape was slightly more elliptical than round. We measured the area and then provided an effective diameter, i.e., the diameter of a circle with the same area as the sample. The photos of the sample with progressively increasing load are shown in Fig. S5.

When one indents a gasket, there is an almost linear pressure gradient from the culet center to the edge of the culet where the pressure drops to very low values. Thus, if a sample like hydrogen is loaded, as pressure is increased, the hole filled with hydrogen not only gets smaller but can migrate from the center of the culet to the edge, if it is slightly off center. That is what happened in this case [see Fig. 1(c)]. In this figure, the load had been increased so that the small sample (diam.  $\sim 3 \mu\text{m}$ ) is at the top edge, indicated by an arrow, and surrounded by Re. Rhenium is also exposed at the lower part of the figure.

Our DACs have diamonds mounted on cylinders that fit snugly in a cylindrical hole (see Ref. 16 for the design). One cylinder is fixed, and the other translates to increase the load when the screw is turned. In our first observation of MH,<sup>10</sup> when the screw was rotated, the pressure increased. Subsequently, in runs with this DAC, at high pressures, when the screw was turned, the load would increase, but sometimes, the pressure would not change until after a few turns, increasing the force, and then the pressure jumped up, while the load measured with the strain gauge partially fell back. At about 240 GPa, with turning of the screw, the pressure increased to the  $\text{H}_2$ -PRE pressure region [see Fig. S6(b)], i.e., above about 360 GPa. With further turning, the sample turned black and, finally, began to shine, that is, it became metallic [see Figs. 1(c) and S5], as was observed by Dias and Silvera. We have traced the sticking problem to pump oil condensed in the warm part of our cryostat that is cryo-pumped onto the DAC and one of the windows. Evidently, this causes the sticking until enough force is applied and the moving cylinder breaks loose and behaves normally.

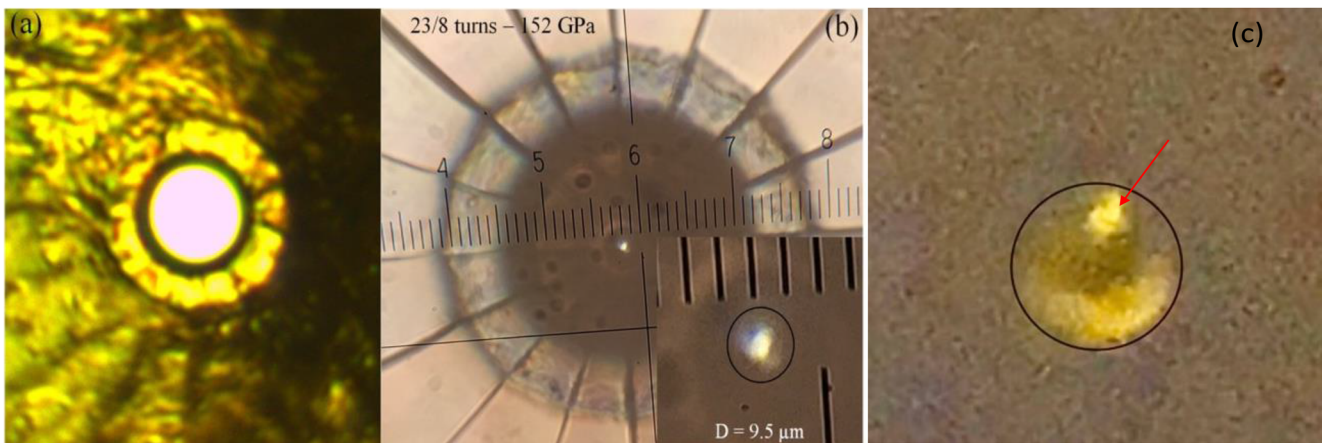


**FIG. 1.** (a) The pre-indented gasket viewed through the Leitz microscope, back and front-lit to show the EDM'd hole; note the black slag at the edge of the hole. (b) The sample under the diamond viewed through the macroscope. This high-resolution image can be zoomed in (inset) to measure the sample hole size. We have superimposed a circle around the  $30 \mu\text{m}$  diameter culet. Note that the sample hole is surrounded by black slag, rather than reflective Re. (c) Photo of MH at a very high pressure (46/8 turns); the arrow points to the sample surrounded by Re.

### III. RESULTS

#### A. Measurement of reflectance

To measure reflectance, one measures a reflected intensity and normalizes to the incident intensity. The incident intensity is challenging to measure in a DAC as the sample cannot be removed. In order to better understand the measurement of reflectance in a DAC, we first studied the reflectance of rhenium in a DAC at room temperature.<sup>17</sup> To measure the reflectance  $R_{ds}$  of the light off the sample,  $s$ , pressed against the diamond,  $d$ , one needs to know the intensity  $I_0$  of the light incident on that surface. We measure the light  $I_d$  reflected off the diamond table and the light  $I_{ds}$  reflected off the MH sample, pressed against the diamond. The incident intensity  $I_0$  propagates into the diamond, reduced by  $R_d$ , the reflectance from the diamond table, and then reflects off the diamond/sample surface. This reflected light is again reduced by  $R_d$  as it emerges out of the table to a detector that measures the intensity. It is easily shown that

$$R_{ds} = \frac{R_d}{(1 - R_d)^2} \frac{I_{ds}}{I_d} e^{2\alpha D}. \quad (1)$$

The exponential term is due to the absorption or scattering of light out of the beam in the diamond of thickness  $D$  and absorption coefficient  $\alpha$ ; the factor of 2 is due to the double pass through the diamond.  $R_d = (n_d - 1)^2 / (n_d + 1)^2$ , where  $n_d = 2.41$  is the index of refraction of diamond in the near-IR.

To measure  $I_d$  and  $I_{ds}$  (see the optical layout in Fig. S7), we used five narrow-band light emitting diodes (LEDs) at wavelengths 625, 720, 810, 890, and 950 nm, obtained from Digi-Key. We avoid LEDs with shorter wavelengths as the diamond absorption increases as the wavelength decreases. It would be useful to extend the range further into the IR where diamond losses are less, but our detector loses quantum efficiency in the 1000 nm region and beyond. The LEDs were mounted on a disk and could be rotated into position on an optical axis. The light was collected with a lens and focused on a pinhole; the emerging light was collimated with a lens and directed into the macroscope to be focused onto the DAC. The optical setup, including the macroscope, was on a platform while the cryostat containing the DAC was on a separate large optical table (see Fig. S7). The distance between the macroscope and the DAC could be finely adjusted with micrometers to focus either on the diamond table or on the culet/sample region. Our study on rhenium in a DAC<sup>17</sup> showed that it is important that the incident light be normal to the plane of the sample. Thus, the cryostat containing the DAC was on a special platform that enabled rotation, tilting, or translation of the cryostat so that the light was normal to the diamond table. The LEDs and DAC had to be carefully aligned to avoid large variations in the measured reflectance. Only light from the 625 nm LED was easily visible to the eye. To align the other LEDs, we placed an IR sensitive camera behind the collimating lens and adjusted the LED until the intensity was symmetric and almost uniform. A satisfactory alignment took several hours.

In this reflectance analysis,  $I_{ds}$  and  $I_d$  are measured; the major unknown is the absorption of the diamond. Vohra<sup>18</sup> studied the opacity of a few types of diamonds under load. At that time, it was thought that the opacity of diamond was due to the closure of a bandgap, but the interpretation of recent studies at SLAC<sup>19</sup> concludes that the gap does not close and the opacity is due to scattering

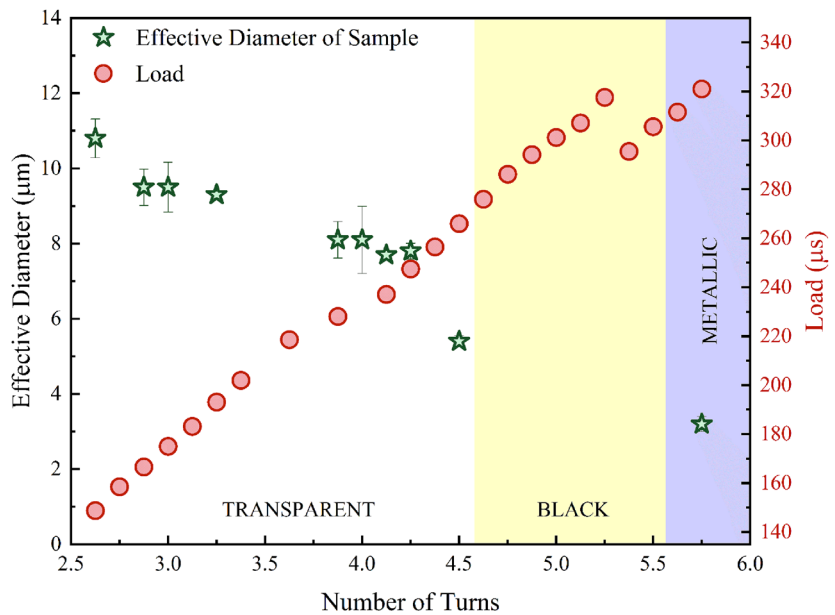
or interaction with impurities. Regardless of the interpretation, we consider the data of Vohra who plots the optical density (OD) of diamond (see Ref. 10, Fig. S5). We extrapolate these data to 500 GPa and then interpolate to find the opacity in the IR (Fig. S8). This indicates that the OD is rather flat in the near-infrared. However, the values of about OD = 1.5 would give unphysical values of reflectance, far greater than 1 in Eq. (1). We believe that our diamonds are of very high quality and would have a lower OD. In our analysis, we used a value of 0.4 for all LEDs, to have a physically acceptable result with reflectance less than 1.

For measurements of the reflected signal, we used a monochrome 1440 × 1080 pixel CMOS camera with 3.45  $\mu\text{m}$  square pixels, model CS165MU, from Thorlabs. It is sensitive in the near-IR, to just beyond 1000 nm. The advantage over a color CMOS is that there are no Bayer filters, so the overall quantum efficiency is greater at any detectable wavelength. In monitoring the progress of the hydrogen sample, it is useful to have a color camera, so we took smartphone photos of the sample at all loads.

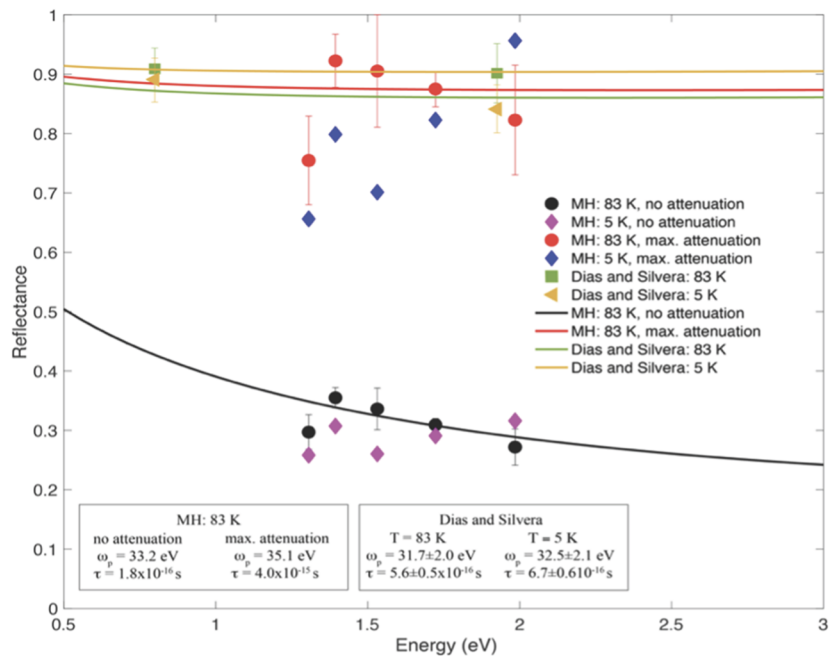
To determine the uncertainty in reflectance, we misaligned the LEDs and then realigned to measure again. This was performed twice at liquid nitrogen temperatures to determine an uncertainty. These uncertainties were used in the fit to the free-electron model. Reflectances were only measured once at helium temperatures, due to the recent liquid helium shortage and limitations on time with a cold cryostat, so that we had enough helium in reserve to study metastability at low temperatures. We are not sure of the uncertainty of reflectance at helium temperatures as we did not have sufficient time (liquid helium) to carry out our usual alignment; these data were not fit.

Figure 2 shows the effective diameter of the sample as a function of load or number of turns. The sample of MH was very small, about 3  $\mu\text{m}$  in diameter. With increasing load, we measured the pressure using the shift of the IR active vibron. This is shown in Fig. S4, where the sample progresses in pressure; at 23/8 turns, it enters phase III (see Fig. S1). At 29/8 turns, the pressure jumped up and the vibron absorption disappeared. The sample had entered into phase H<sub>2</sub>-PRE. In Fig. S6, we show the fall off of the integrated intensity, similar to observations made in Fig. 2(c) of Ref. 7; this corresponds to the closing of the electronic gap.

The measured reflectance at liquid nitrogen and liquid helium temperatures is shown in Fig. 3, where we fit the reflectance data measured at liquid nitrogen temperature with a Drude free-electron model (the lower black curve with black solid circle data points). This fit has a plasma frequency of 33.2 eV, consistent with atomic metallic hydrogen,<sup>1</sup> while the scattering time  $\tau$  is much longer than that found by Dias and Silvera, perhaps indicating fewer scattering centers in the sample. Over our spectral range, the reflectance was between 0.3 and 0.4, much lower than the reflectance (between 0.8 and 0.9) observed by Dias and Silvera. This difference is attributed to the absorption of light by the diamond, and the uncertainties in the fitting are dominated by the modeling of the diamond absorption, as shown in the data boxes in Fig. 3. As mentioned above, we modeled the diamond absorption with an OD of 0.4 and find reasonable agreement with previous measurements of Dias and Silvera, also shown in Fig. 3. The basic trend is for the reflectance to increase as the photon energy decreases. The data confirm that MH has been reproduced. We determined the pressure by the extrapolation of data shown in Fig. S4; this yielded 477–491 GPa for the pressure



**FIG. 2.** The effective diameter of the hydrogen sample as a function of number of turns of the screw or load. The screw was turned up by eighths of a full turn, for a total of almost six full turns. The sample progressed from transparent to black to metallic. A kink in the load (red points) usually corresponds to a jump in pressure.



**FIG. 3.** Reflectance of MH as a function of photon energy. The lower curve with black solid circles is the measured data. In the upper curves, we compared the measurements with those by Dias and Silvera by modeling the attenuation of light by the diamonds. Uncertainties and correction factors are discussed in the text. Data at helium temperature are shown but were not optimized and not fit. The pressure was estimated to be in the range 477–491 GPa.

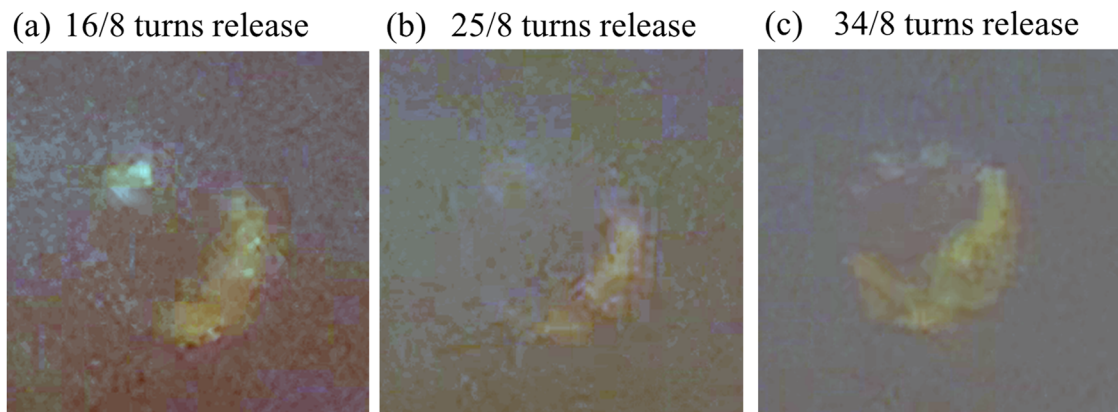


**FIG. 4.** Observation of the sample while the load is released, using a smartphone camera. (a) We could still observe the MH, near the upper edge of the culet. (b) Sample escaped and hole closed while under load. (c) Load or pressure on the gasket is zero.

when MH appeared, in agreement with other measurements of the metallization pressure.

### B. Metastability

To test for metastability, we illuminated the sample from both front and back at 5 K. Both a smartphone camera and the CMOS camera were mounted on the eyepieces of the microscope and set to run continuously (smartphone:  $\sim 30$  Hz frame rate; CMOS  $\sim 20 - 35$  Hz) as the load was reduced in steps of 1/8 turn. Ideally, if metastable, we would see the MH sample at zero pressure and then raise the temperature until it converted to molecular hydrogen. For convenience, we zero'd the strain gauge meter (set 46/8 turns to zero, Fig. 2) and measured the release of strain as the load was reduced. In Fig. 4, at 16/8 turns release, we could still see the MH, indicating that it is metastable. However, with more turns, the shiny sample disappeared (between 23/8 and 25/8 turns release), and the hole closed, as we saw no transmitted light. The shiny lower part of the figure is Re. The fact that the hole closed indicates that there was still a load on the sample when it escaped (see comment S9). We continued to release the load to make sure that the pressure was zero and diamonds were no longer compressing the gasket. At this time, we can claim with no uncertainty that MH is not metastable at zero pressure.

### C. Conclusions and perspectives

In this experiment, we have reproduced metallic hydrogen in the laboratory at a pressure in the range 477–491 GPa, in good agreement with other measurements. When releasing the load, we have shown that MH is not metastable when the pressure is reduced to zero. This is not the end of the quest for metastability at zero pressure. In the future, we plan to metalize deuterium and study its possible metastability.

### SUPPLEMENTARY MATERIAL

We provide further information in Supplementary Online Material or the supplementary material. This file provides the reader

with the convenience of seeing, for example, the figures of the phase diagram or the figures of hydrogen at various stages of pressure, etc., published elsewhere. Moreover, we provide unpublished data, such as the tendency of laser power to cause diamond failure, pressure calibration data, optical setups, as well as the photos of hydrogen under pressure in the current experiment.

### ACKNOWLEDGMENTS

This research was supported by the SSAA of the DoE with Grant Nos. DE-NA0003917 and DE-NA0004087 and BES Grant No. DE-SCF0020303 and by the NSF, Grant Nos. DMR-190594 and DMR-1809649. This work was performed, in part, at the Harvard University Center for Nanoscale Systems (CNS), a member of the National Nanotechnology Coordinated Infrastructure Network (NNCI), which is supported by the National Science Foundation under NSF Award No. ECCS-2025158. K.L. received partial support from an HCRP (Harvard College Research Program) grant.

### AUTHOR DECLARATIONS

#### Conflict of Interest

The authors have no conflicts to disclose.

#### Author Contributions

**W. C. Ferreira:** Data curation (equal); Investigation (equal); Resources (equal); Writing – review & editing (equal). **M. Möller:** Data curation (equal); Formal analysis (equal); Methodology (equal); Software (equal); Writing – review & editing (equal). **K. Linsuain:** Data curation (equal); Investigation (equal); Writing – review & editing (equal). **J. Song:** Conceptualization (equal); Methodology (equal); Writing – review & editing (equal). **A. Salamat:** Conceptualization (equal); Writing – review & editing (equal). **R. Dias:** Conceptualization (equal); Writing – review & editing (equal). **I. F. Silvera:** Conceptualization (equal); Data curation (equal); Funding acquisition (equal); Supervision (equal); Writing – original draft (equal).

## DATA AVAILABILITY

The data that support the findings of this study are available from the corresponding author upon reasonable request.

## REFERENCES

- <sup>1</sup>I. F. Silvera and R. Dias, *J. Phys: Condens. Matter* **30**, 254003 (2018).
- <sup>2</sup>E. G. Brovman, Y. Kagan, and A. Kholas, Sov. Phys. JETP **34**, 1300 (1972).
- <sup>3</sup>E. Babaev, A. Sudbo, and N. W. Ashcroft, *Nature* **431**, 666 (2004).
- <sup>4</sup>C. M. Tenney, K. L. Sharkey, and J. M. McMahon, *Phys. Rev. B* **102**, 224108 (2020).
- <sup>5</sup>S. N. Burmistrov and L. B. Dubovskii, *Low Temp. Phys.* **43**, 1152 (2017).
- <sup>6</sup>G. J. Ackland, [arXiv: 1709.05300v1](https://arxiv.org/abs/1709.05300v1) (2017).
- <sup>7</sup>R. Dias, O. Noked, and I. F. Silvera, *Phys. Rev. B* **100**, 184112 (2019).
- <sup>8</sup>M. Zaghou, A. Salamat, and I. F. Silvera, *Phys. Rev. B* **93**, 155128 (2016).
- <sup>9</sup>E. Wigner and H. B. Huntington, *J. Chem. Phys.* **3**, 764 (1935).
- <sup>10</sup>R. Dias and I. F. Silvera, *Science* **355**, 715 (2017).
- <sup>11</sup>I. F. Silvera and R. Dias, [arXiv:1703.03064](https://arxiv.org/abs/1703.03064) [Cond-mat] (2017).
- <sup>12</sup>R. Dias, A. Salamat, and I. F. Silvera (2022) (submitted)
- <sup>13</sup>I. F. Silvera and R. Dias, *Adv. Phys.: X* **6**, 1 (2021).
- <sup>14</sup>M. I. Eremets, V. S. Minkov, P. P. Kong, A. P. Drozdov, S. Chariton, and V. B. Prakapenka, *Nat. Commun.* **14**, 907 (2023).
- <sup>15</sup>C. Narayana, H. Luo, J. Orloff, and A. L. Ruoff, *Nature* **393**, 46 (1998).
- <sup>16</sup>I. F. Silvera and R. J. Wijngaarden, *Rev. Sci. Instrum.* **56**, 121 (1985).
- <sup>17</sup>J. Song, I. Chuvashova, and I. F. Silvera, *Appl. Phys. Lett.* **120**, 011601 (2022).
- <sup>18</sup>Y. K. Vohra, in Proceedings of the XIII AIRAPT International Conference on High Pressure Science and Technology (Bangalore, India, 1991).
- <sup>19</sup>E. J. Gamboa *et al.*, *SLAC-PUB-16488*, 2017.

## Supplementary Information

### Metallic Hydrogen: Experiments on Metastability

W. Ferreira<sup>1</sup>, M. Møller<sup>1</sup>, K. Linsuain<sup>1</sup>, J. Song<sup>1</sup>, A. Salamat<sup>2</sup>, R. Dias<sup>3</sup>, and I. Silvera<sup>1</sup>  
<sup>1</sup>Lyman Laboratory of Physics, Harvard University, <sup>2</sup>Dept. of Physics and Astronomy, University of Las Vegas, Nevada, and <sup>3</sup>Dept. of Physics and Astronomy, Univ. of Rochester

Our supplementary information consists of a collection of figures, shown below.

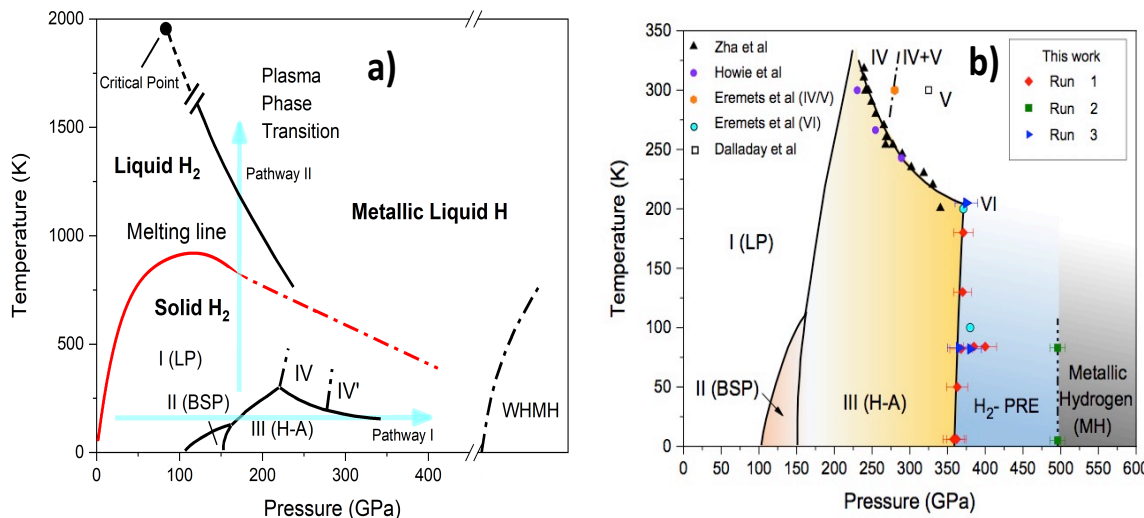


Fig. S1. The pressure/temperature phase diagram of hydrogen from Ref. [2] a) The high temperature phase diagram showing Pathways I and II to atomic MH. b) An expanded view of Pathway I, showing several phases within the molecular solid, encountered with increasing pressure.

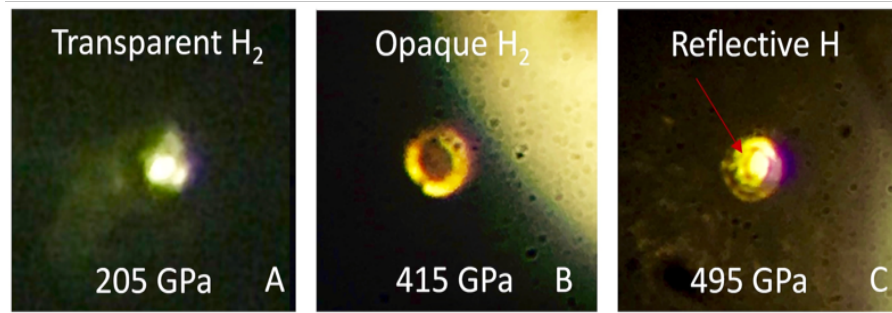


Fig. S2. A figure from Ref. [1] showing hydrogen at various pressures, including MH in C. The sample is back lit in all figures, but B and C are non-transmitting. A is only back lit, while B and C are also front lit.

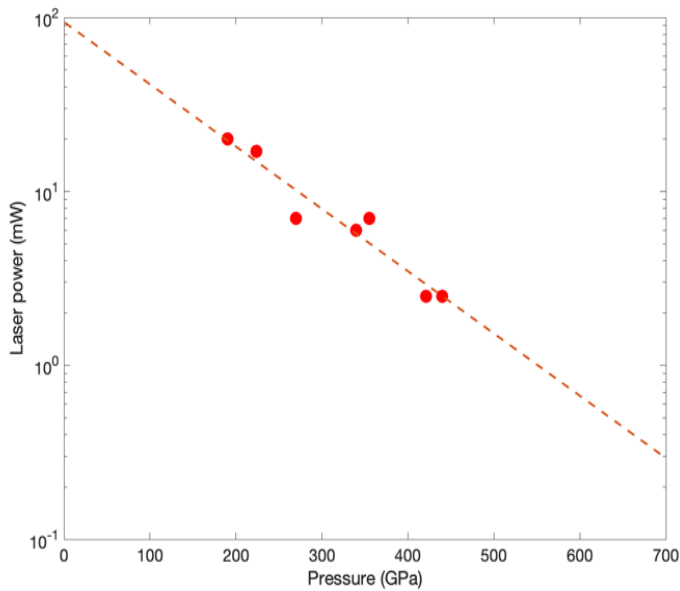


Fig. S3. Laser power focused into the stressed region of the diamond, causing diamond failure versus pressure of the sample. This is indicative of the problem; we have also found that pressure could be measured with higher power without failure of the diamonds (not shown on this graph).

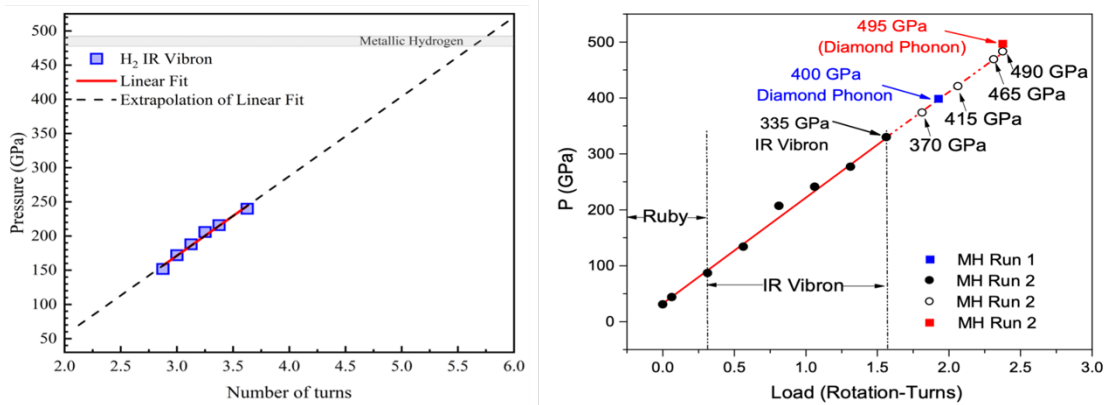


Fig. S4. Pressure versus load or number of turns of drive screw. Left panel: the current experiment with extrapolation. Right panel: similar to left panel but earlier experiment from Ref. [1] showing that the extrapolation is confirmed by measurement of the shift of the diamond phonon.

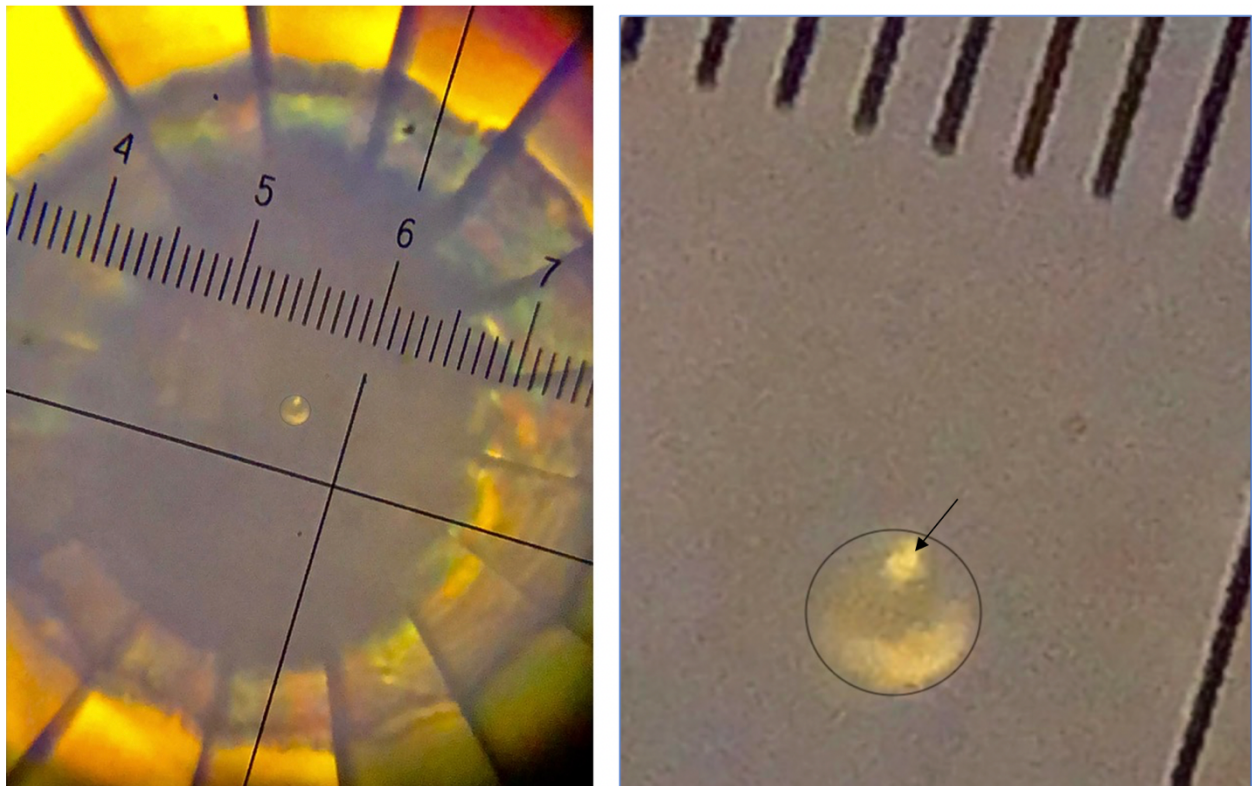
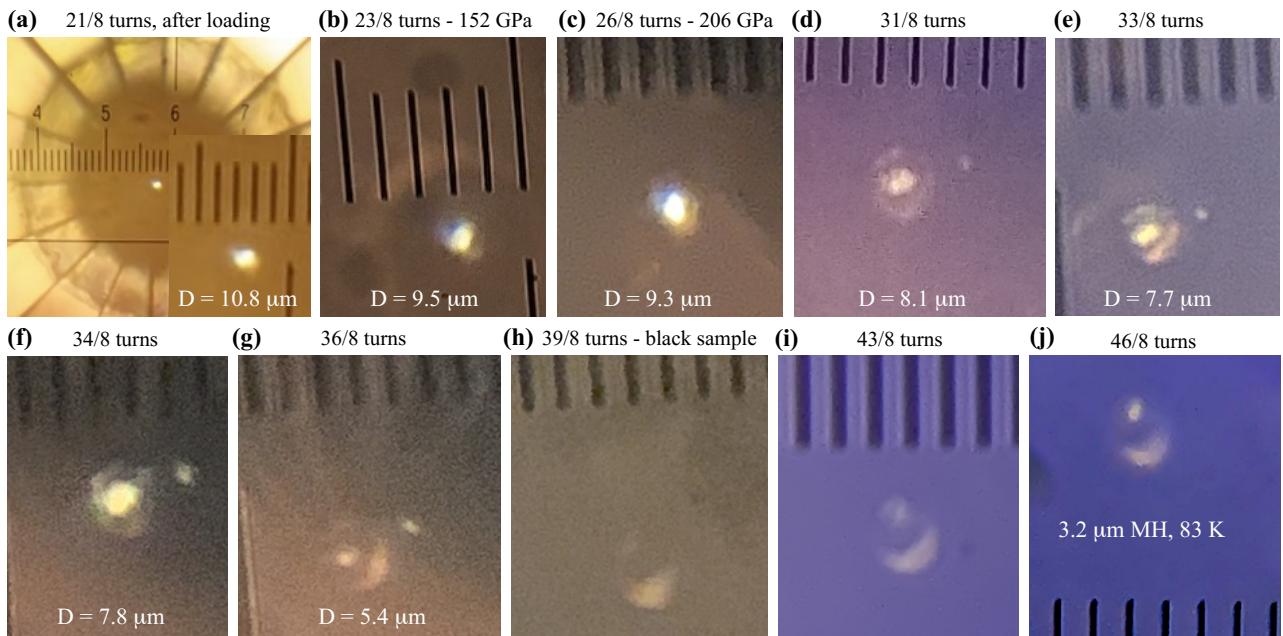
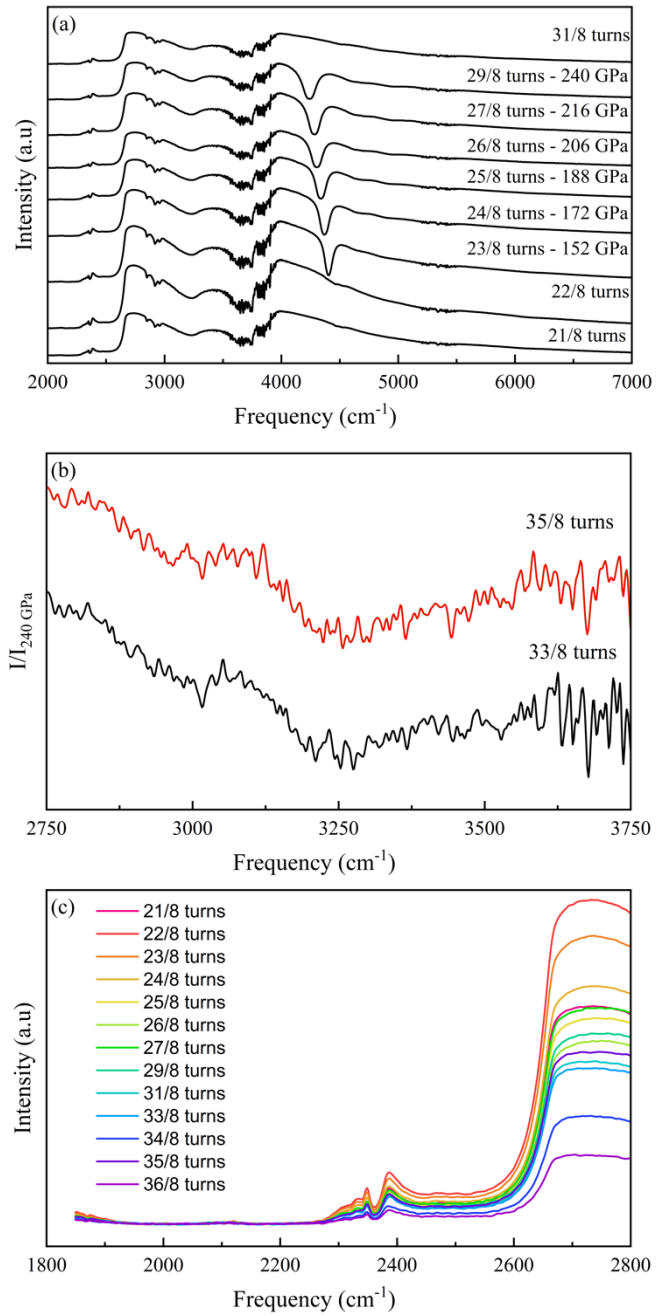


Fig. S5. Photos of the sample with increasing load (turns), corresponding to regions shown in Fig. 2. The upper figure: This shows the progression of the sample as the load was increased. For lower number of turns the sample is surrounded by black slag. With increasing load (e), both the sample and Re are observed. In h) the sample is black and blends in with the black slag. Finally, in j) the sample becomes metallic and shines; in the lower region of the culet the shiny surface is Re. The lower figure: This shows another picture of the MH, blown up on the right. A circle is drawn around the diamond culet and an arrow points to the MH, surrounded by Re.



**Figure S6.** Infrared observations of pressure in the sample. a) This shows the vibron spectrum up to 240 GPa in phase III (see Fig. S1). b) The pressure jumps and the sample enters the  $\text{H}_2$ -PRE phase. c) This shows the integrated intensity in the IR demonstrating that the pressure is increasing as the load increases. Comparable results were observed in Ref. [1], Fig. 2.

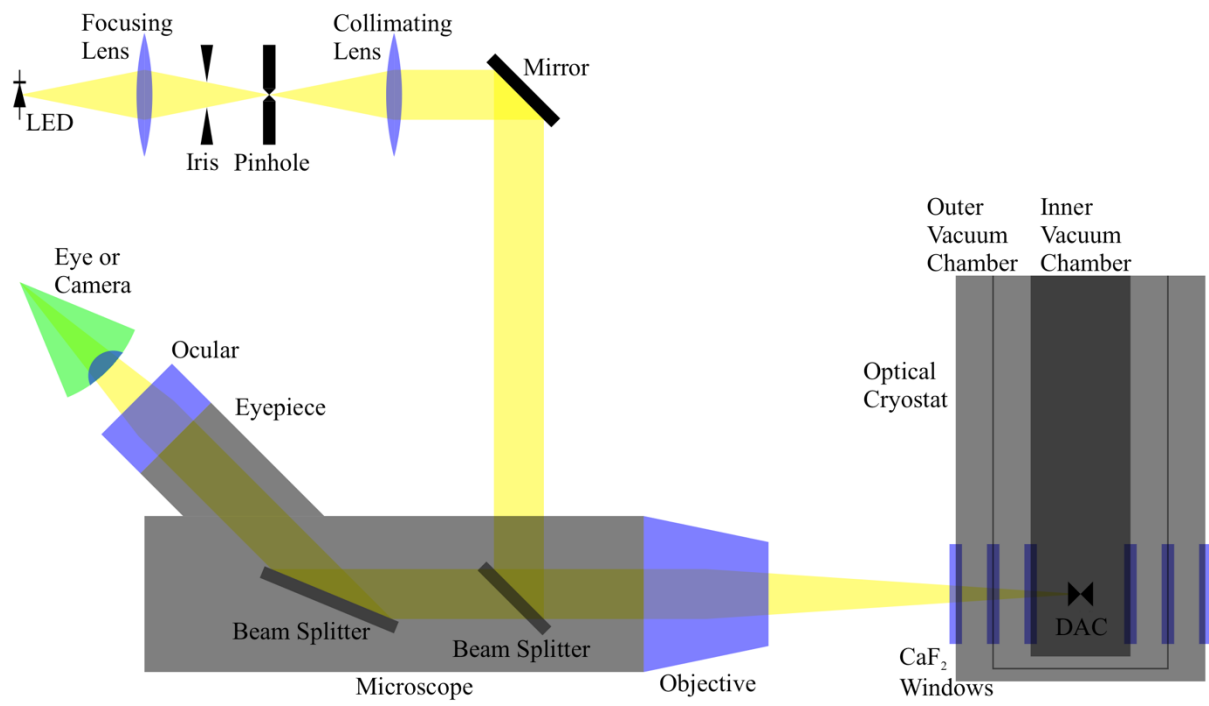


Fig. S7. The optical layout used for measuring the reflectance. Cameras could be mounted on the eyepieces of the microscope, with or without the ocular.

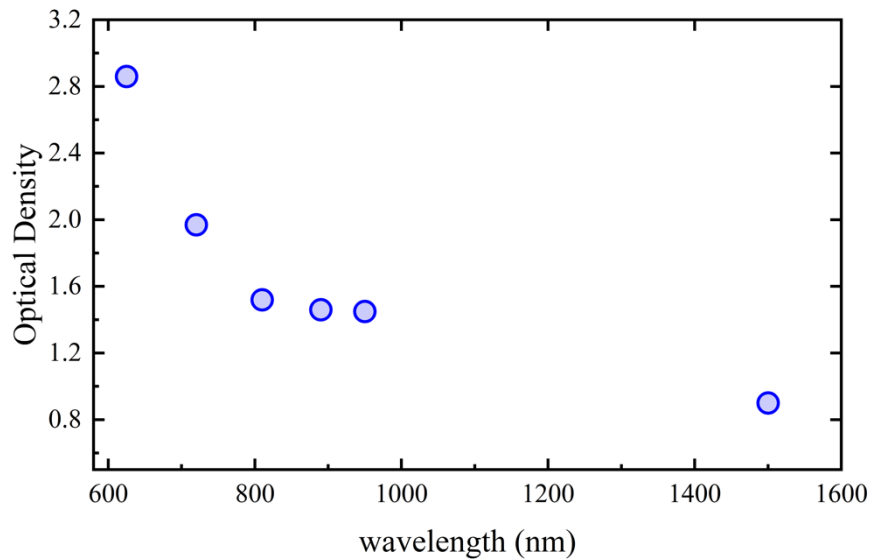


Fig. S8. The optical density extrapolated from Vohra's paper, described in the text.

S9. With increasing pressure, the pressure vs turns scale shown in Fig. S4 is valid. In this case, part of the load causes the thinning gasket to flow out in contact with the diamond bevel and provides support of the diamond. However, in reducing the load the part of the gasket providing support on the bevel releases and the confined sample can leak out or evaporate out while there is still a substantial load. With no sample in the hole the load can cause the hole to close. We have observed this behavior in earlier experiments on molecular hydrogen as the pressure was reduced.

## References

- [1] R. Dias and I. F. Silvera, *Science* **355**, 715 (2017).
- [2] R. Dias, O. Noked, and I.F.Silvera, *Phys.Rev. B* **100**, 184112 (2019).